ADVANCED MATERIALS

Polymer Network–Stabilized Liquid Crystals**

By Ingo Dierking*

The fabrication and properties of polymer network–stabilized liquid crystals, formed by polymerization of a small amount of a bifunctional photoreactive monomer dissolved in a liquid-crystalline phase, are reviewed. The polymer network morphology is strongly related to preparation conditions such as monomer content, polymerization temperature, and ultraviolet (UV) curing conditions. The transfer of anisotropic liquid-crystalline order onto the network is discussed in detail. The electro-optical performance of network-stabilized nematics, cholesterics, and ferroelectric smectics is largely dependent on the morphology of the network, as will be demonstrated with an emphasis laid on polymer-stabilized cholesteric textures (PSCTs). A general correlation between polymerization conditions, network morphology, and electro-optical behavior will be outlined and aspects concerning applications discussed.

1. Introduction

1.1. Liquid Crystals

Liquid crystals (LCs) are anisotropic fluids, combining the flow properties of an ordinary liquid with the anisotropic physical parameters generally only found for crystals. They represent thermodynamically stable phases situated between the ordinary isotropic liquid and the crystalline solid, differing in their degree of order. We generally distinguish between thermotropic phases, which are observed solely by temperature variation (at constant pressure) and lyotropic phases, which are formed by addition of an isotropic solvent, the concentration of the solution being the essential variable of state. The latter will not be discussed within the scope of this review. Thermotropic mesophases are further distinguished by the shape of their constituent molecules: calamitic for rod-like, discotic for disk-like, and sanidic for lath-like molecular shape. Here we will only discuss phases formed by calamitic molecules.

The simplest of the liquid-crystalline phases with the lowest order and thus the highest symmetry is the nematic mesophase, which exhibits only orientational order along the long molecular axis (the director), the centers of mass being isotropically distributed (Fig. 1a). If the constituents of this phase are chiral molecules, a spontaneous twist with the helical axis perpendicular to the local director is observed and we speak of the chiral nematic or cholesteric phase (Fig. 1b). The introduction of one-dimensional positional order results in the formation of smectic mesophases, which exhibit a layered structure. For fluid smectics the centers of mass within a smectic layer are still isotropically distributed. For the smectic A (SmA) phase the director points along the smectic layer normal (Fig. 1c), while in the smectic C (SmC) phase it makes an angle, the so-called tilt angle θ, which is generally a temperature-dependent quantity (Fig. 1d). From symmetry considerations it has been shown that all tilted smectics comprised of chiral molecules (*) exhibit a spontaneous polarization;[1] they are thus pyroelectric. For some mesophases, especially the SmC* phase, the direction of this polarization can be reversed by application of an electric field and we speak of (improper) ferroelectric liquid crystals (FLCs). For a detailed overview on liquid crystals and their properties we refer to the monographs.[2–6]

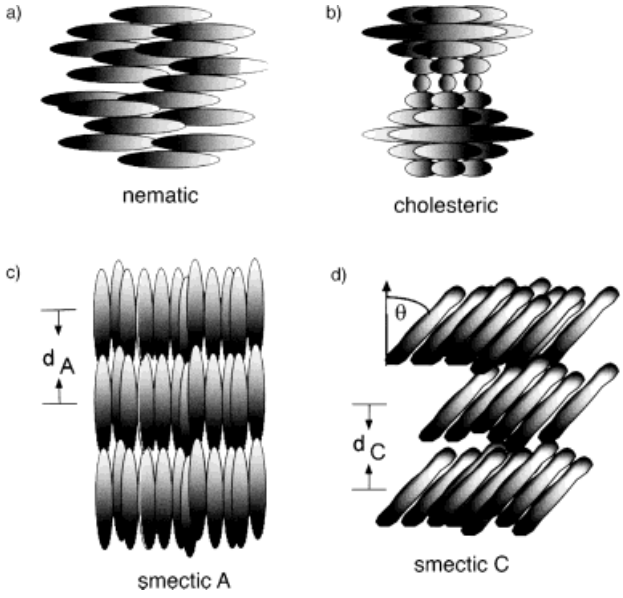

Fig. 1. Schematic structural representation of different liquid-crystalline phases from calamitic molecules. a) Nematic, b) cholesteric or chiral nematic, c) smectic A, and d) smectic C phase.

[*] Dr. I. Dierking
Institut für Physikalische Chemie
TU Darmstadt
Petersenstrasse 20, D-64287 Darmstadt (Germany)

[**] I acknowledge valuable discussions with L.-C. Chien, G. A. Held, L. L. Kosbar, S. T. Lagerwall, A. C. Lowe, M. A. Osipov, D.-K. Yang, and S. Zumer. I also thank W. Haase for financial support.

  0935-9648/00/0302-0167 $ 17.50+.50/0

1.2. Polymer–Liquid Crystal Dispersions

Polymer–liquid crystal dispersions have attracted great interest over the last years, firstly because of their potential as light shutters, privacy windows, or novel, paper-like reflective displays, but also in the study of fundamental physical questions, such as liquid-crystalline order and director configurations in confined geometries or phase transitions.[7,8]

1.2.1. Polymer-Dispersed Liquid Crystals

Polymer-dispersed liquid crystals (PDLCs) are composite materials where a rather small amount of a liquid crystal (≈30 %) is embedded in a continuous polymer matrix, usually forming LC droplets with a diameter on the order of several micrometers. Generally, two fabrication methods can be used: encapsulation and phase separation. The former method was introduced by Fergason[9] and Drzaic,[10] who dried a polymer solution (polyvinyl alcohol) with emulsified LC droplets. The latter method was reported by Doane et al.[11] in 1986. It involves initiating phase separation by thermally curing the polymer precursor. Other phase separation methods have been described since, such as evaporation of a solvent from a polymer–liquid crystal mixture,[12] temperature-induced phase separation of a polymer–liquid crystal mixture on cooling,[13] or, by far the most popular technique today, by photopolymerization of a mixture of a polymer precursor with a LC.[14]

From the viewpoint of basic research the process of phase separation during polymerization in an anisotropic medium is of special interest, and has been addressed in several publications.[15–17] Also phase transitions and the nematic order parameter are greatly influenced by confinement of the LC to small droplets.[18] The operation principle of the classic PDLC device using a nematic LC[19] is simple: in the field-free state the average optical axis of the confined nematic in different droplets is isotropically oriented and the device is strongly light scattering. Application of an electric field causes a reorientation of the nematic director in each droplet such that the optical axis is aligned parallel to the field vector (for a LC with positive dielectric anisotropy). If the refractive index along the long molecular axis is matched with that of the polymer matrix, the device is transparent in the field-on state. Other display devices based on cholesteric LCs with selective reflection in the visible wavelength region have been realized.[20] Also the use of FLCs in PDLCs has been proposed.[21] For a more detailed overview on PDLCs we refer to Chapter 8 of the book *Liquid Crystals in Complex Geometries*[8] and review articles by Kitzerow[22] and Bouteiller and Barny.[23]

1.2.2. Polymer-Stabilized Liquid Crystals

At the opposite end of the phase diagram, at large LC concentrations, we speak of polymer-stabilized liquid crystals (PSLCs). Here, the liquid-crystalline material represents the continuous matrix, while a small amount (≈5 wt.-%) of a crosslinked polymer is dispersed in the anisotropic fluid. The general idea of PSLCs is the stabilization of alignment of a low-molecular-mass LC by elastic interactions between the network and LC. These systems promise potential in direct view reflective display applications. Their fabrication implies an understanding of the relationship between monomer constitution, polymerization conditions, network morphology, and electro-optical performance. Fundamental research interests again lie in the process of polymerization, the transformation of liquid-crystalline order onto the polymer network, phase transitions in randomly disturbed systems, and effects of networks on local phase symmetry of LC phases. In the following, these systems will be discussed in detail.

2. Polymer Network–Stabilized Liquid Crystals

2.1. Materials

Pioneering work on the synthesis of functionalized photoreactive liquid-crystalline monomers used for the fabrication of PSLCs was carried out by Broer and co-workers at Philips.[24–28] The monomers used in today's PSLCs are often based on acrylate or methacrylate functional groups attached to both sides of the mesogenic core by a flexible alkyl chain. Some examples, also of commercially available compounds (Merck), are given in Figure 2.

Ingo Dierking received his Dr. rer. nat. in 1995 from the Institute of Physical Chemistry at the Technical University of Clausthal, Germany. After a one year post-doctoral appointment at the IBM TJ Watson Research Center in Yorktown Heights, NY, where he worked on reflective displays, he joined the Department of Physics at Chalmers University of Technology in Gothenburg, Sweden as a Feodor Lynen Fellow of the Alexander von Humboldt Foundation (1997–1999). In 1999 he was appointed "docent" (associate professor) there. Currently he is an associate lecturer at the Institute of Physical Chemistry at Darmstadt University of Technology, Germany. His research interests include polar effects in liquid crystals, polymer network–stabilized systems, frustrated smectic phases, smectic layer instabilities, and dispersions of colloidal particles in anisotropic fluids.

  0935-9648/00/0302-0168 $ 17.50+.50/0

ADVANCED MATERIALS

2.2. Methods of Fabrication

To make a PSLC device, generally a room-temperature LC is mixed with a photoreactive bifunctional monomer at a concentration ratio of approximately 90–95 wt.-% LC/10–5 wt.-% monomer, with a small amount of photoinitiator (often benzoinmethylether) added. Under yellow light conditions this mixture is filled into test cells consisting of indium tin oxide (ITO) coated glass substrates with additional rubbed alignment layers (often polyimide or nylon), either by capillary action or vacuum filling. The material is then brought into the desired orientation by surface interactions and/or the application of electric or magnetic fields and photopolymerization is induced by irradiation of the sample with UV light of moderate intensity for several hours. During the polymerization process (often a radical chain polymerization) phase separation of the polymer from the LC matrix occurs, as can be confirmed by infrared (IR) spectroscopy, scanning electron microscopy (SEM), and neutron scattering.[29] The basic idea of introducing a polymer network into the LC matrix is a transfer of the orientational order of the mesophase to the polymer network during polymerization, and thus the stabilization of the original texture by introduction of a large surface to volume ratio as compared to simple orientation by substrate alignment. Figure 3 schematically summarizes this process.

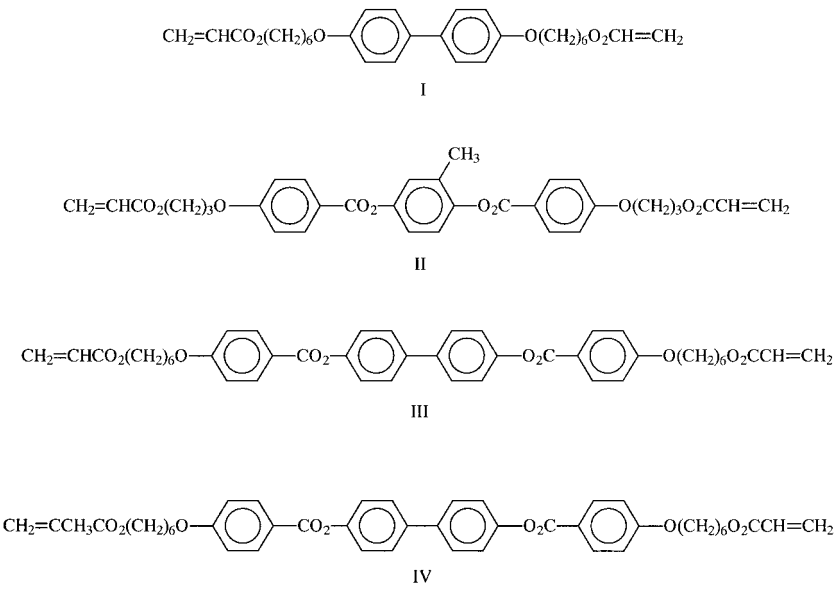

Fig. 2. Selection of some bifunctional photoreactive monomers used in the fabrication of polymer-stabilized LCs.

2.3. Polymer Network–Stabilized Nematics

Nematic LCs, stabilized by a polymer network, were the first materials to be investigated in detail.[30–33] Generally, they are formed by photopolymerization of a small amount of reactive bifunctional monomer within the nematic liquid-crystalline state. The texture of the nematic is not influenced by the formation of the network, but application of an electric field results in scattering of light. This light scattering is due to the presence of the network, keeping LC molecules in the vicinity of the polymer strands in their original orientation, while the bulk material reorients under field application.

2.3.1. Network Morphology

During photopolymerization the order of the nematic phase is templated by the forming polymer network; this has been demonstrated by SEM after removal of the LC by a suitable solvent. The network consists of polymer strands oriented along the direction of the director. This has not only been shown for a nematic oriented under planar boundary conditions (director in the plane of the substrate),[31] but also nicely by a side view of homeotropic cells (director perpendicular to the substrates),[34,35] where the polymer strands are oriented from the top to the bottom glass plate.

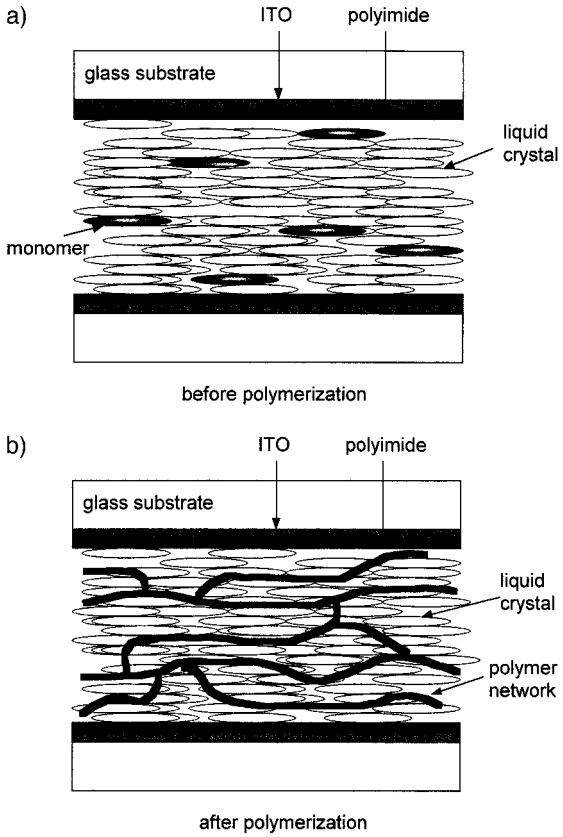

Fig. 3. Schematic illustration of the fabrication of PSLCs. a) Photoreactive monomers dissolved in a LC before polymerization. b) Polymer network stabilizing the LC orientation after polymerization by UV irradiation.

  0935-9648/00/0302-0169 $ 17.50+.50/0

2.3.2. Effect on Physical Parameters

The most striking effect of the polymer network on the LC is that of a residual birefringence, which can be observed well into the isotropic phase[30] and which also allows indirect imaging of the polymer network when viewed in a polarizing microscope. It was shown that a small but nearly constant birefringence (on the order of $\Delta n = 0.01$) is induced by ordering of liquid-crystalline molecules along the network strands up to several tens of degrees into the isotropic phase.[30,36,37] Close to the transition into the nematic phase strong pretransitional ordering is observed by birefringence measurements[36] as well as order parameter determination by nuclear magnetic resonance (NMR).[38,39] Figure 4 depicts exemplary measurements of the residual birefringence as well as the pretransitional behavior on approaching the nematic phase from the isotropic liquid.[36] The birefringence of the polymer–liquid crystal system can be written as $\Delta n = \Delta n_P + \Delta n_{LC}$, where Δn_P is the birefringence contribution of the polymer network and Δn_{LC} that of the LC. From independent measurements of the polymer in an isotropic solvent, Δn_P is determined to be on the order of 0.001, and is approximately independent of temperature. Thus the residual birefringence determined in the isotropic phase can largely be attributed to ordering of the LC molecules due to the polymer network. A more elaborate theoretical treatment based on an order parameter distribution around polymer network strands[8] then allows for an estimation of the (average) radius of the network fibers. It should be mentioned, though, that these values strongly deviate from those observed by SEM.

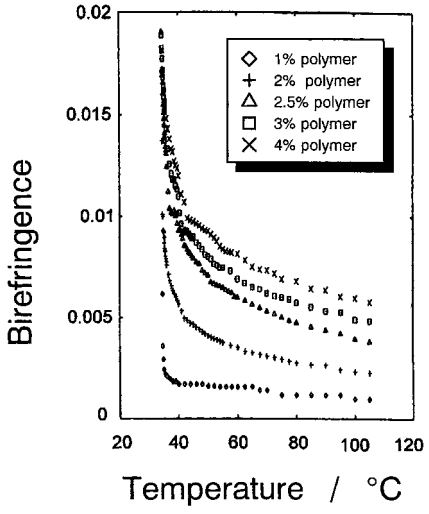

Fig. 4. Birefringence as a function of temperature and polymer network concentration, demonstrating a residual birefringence, induced by the network far into the isotropic phase. Pretransitional effects are very pronounced in the vicinity of the transition to the nematic phase when cooling from the isotropic liquid (data after [36]).

During application of an electric field, the reduction of the birefringence appears at much larger threshold fields as compared to the non-stabilized material[30] and an increasing residual birefringence is observed for increasing polymer content,[31,36,37] while the rotational viscosity remains largely unaffected.[40] Molecular relaxations were found to decrease in frequency and broaden when the polymer content is increased.[41] A similar effect is observed for the phase transition from isotropic to nematic, where the first-order transition is smeared out and the change in enthalpy reduced for increasing polymer concentration.[31] This behavior is attributed to molecules that are already ordered nematic-like by the network in the isotropic phase not contributing to the transition enthalpy. Analogous results were reported for the formation of polymer networks in the SmA phase.[42]

2.3.3. Electro-optics, Stabilized Twisted Nematic and Supertwisted Nematic Devices

From the applicational viewpoint it is desirable to reduce the operational voltage of twisted nematic (TN) devices. This is generally done by the use of nematics with high dielectric anisotropy and small elastic constants at the cost of problems associated with image sticking or increase of the molecular pretilt at the substrates, which involves undesirable substrate preparation techniques. By introduction of a polymer network formed under applied electric field conditions a reduction in driving voltage without alteration of the electro-optical performance (response time) of the TN cell could be achieved.[43]

Supertwisted nematic (STN) devices have their steepest electro-optical response for a twist of 270°, which can only be achieved without the unwanted formation of striped domains by costly substrate preparation techniques. It was shown[44] that the addition of a small amount of polymer network, cured under applied electric field, could be used to suppress the formation of striped domains, even when standard substrate preparation techniques were used.

2.4. Polymer Network–Stabilized Cholesteric Textures

Polymer-stabilized cholesteric textures (PSCTs) are formed by UV-induced polymerization of photoreactive monomers in a chiral nematic or cholesteric phase. In contrast to common LC displays, which operate on the basis of field-induced changes of the birefringence, polymer-stabilized cholesteric textures are based on light scattering, and thus have the advantage that they can be operated without the use of polarizers. Depending on the texture of the field-on and -off state we distinguish between a *normal*-mode and a *reverse*-mode device.[45] In the normal-mode cell the light scattering focal-conic texture is stabilized in the field-off state and a transition to the homeotropic orientation (long molecular axis parallel to the direction of light propagation) is induced by application of electric fields. Switching thus occurs from scattering to transparent or, by use of an appropriate background, from white to black. In a reverse-mode cell the initial planar orientation (helical axis

  0935-9648/00/0302-0170 $ 17.50+.50/0

ADVANCED MATERIALS

perpendicular to the substrates) of a long pitch cholesteric (P = several micrometers) is stabilized by the network and a texture transition to the scattering focal-conic state is induced by electric fields. After field removal the polymer network causes a rapid reorientation back to the planar configuration. Switching by electric field application thus occurs from transparent to scattering, or black to white. The general operation principle and a test cell of a reverse-mode PSCT are shown in Figures 5 and 6, respectively. In the following we will discuss the electro-optical performance of reverse-mode cells in relation to the polymer network morphology obtained under varying curing conditions.

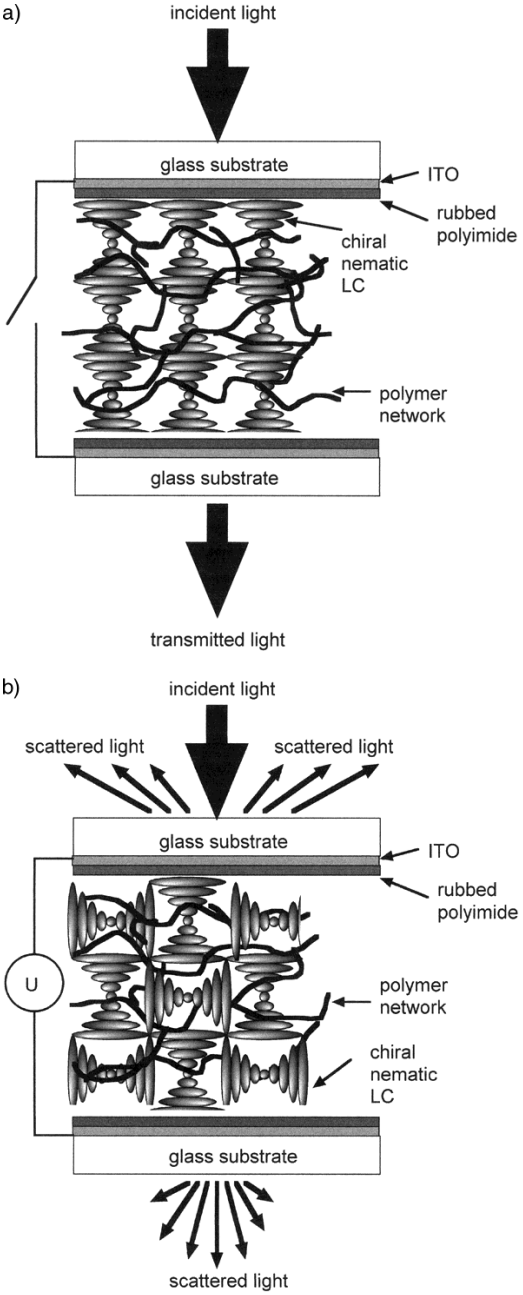

Fig. 5. Functional principle of a PSCT in the reverse mode. a) Transparent (black) in the field-off state and b) scattering (white) for applied voltages. Switching is based on a texture transition from planar to focal-conic.

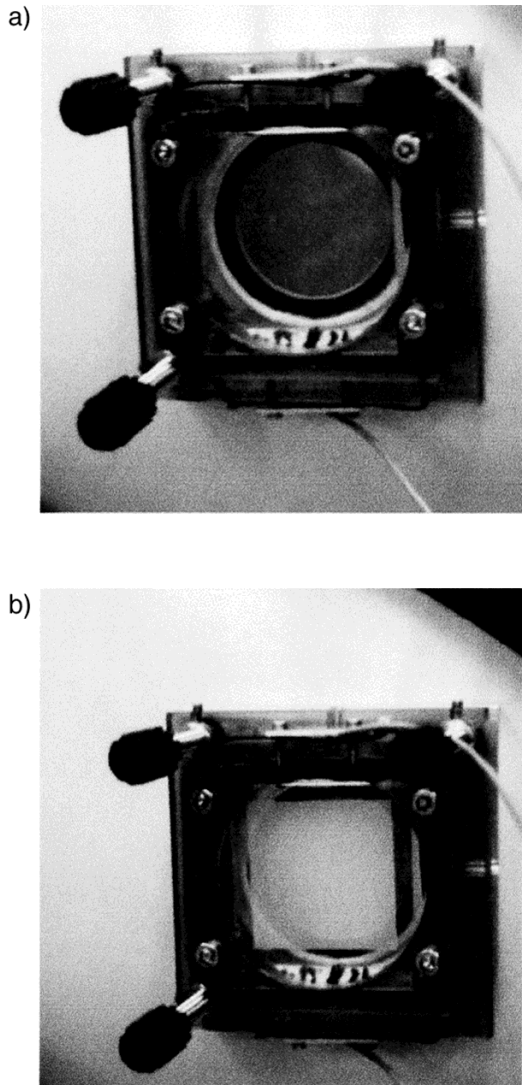

Fig. 6. Demonstration of a reverse-mode PSCT test cell in a) the field-off (transparent) and b) the field-on (scattering) state.

2.4.1. Electro-optical Performance

The general electro-optical response of a reverse-mode PSCT is shown in Figure 7 for the diffuse reflectivity (off-specular back-scattering) in the static case as a function of applied voltage and for its dynamics. Starting in the transparent state at low reflectivity, the voltage is increased until the threshold for the texture reorientation is reached. During the texture transition the reflectivity increases until it saturates at higher voltages. A further increase of the electric field amplitude would result in a transition to the homeotropic orientation and a subsequent decrease in reflectivity (not shown). The reflectivity naturally increases with increasing cell gap and is slightly dependent on wavelength, increasing as the wavelength is shifted from red to blue. The concentration of the added photoinitiator does not have a crucial influence on the electro-optical performance up to rather large values of about 10 wt.-% of the

  0935-9648/00/0302-0171 $ 17.50+.50/0

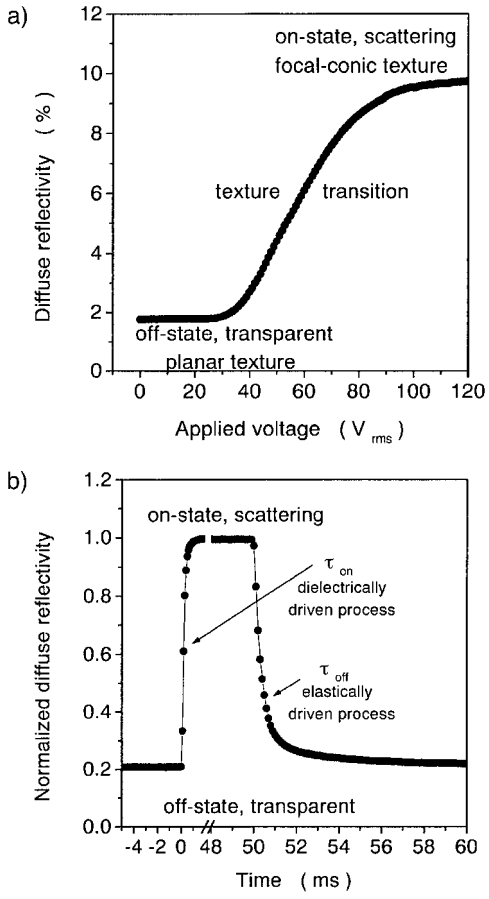

Fig. 7. General electro-optical response of a PSCT in the reverse mode. a) Diffuse reflectivity (back scattering) as a function of applied voltage. b) Dynamic response on application of a pulsed voltage.

monomer content. The exemplary data in Figure 8 summarize this behavior. The principal electro-optical performance parameters such as threshold voltage, reflectivity, and response time of PSCTs strongly depend on the morphology of the dispersed network, which in turn depends on the polymerization conditions.

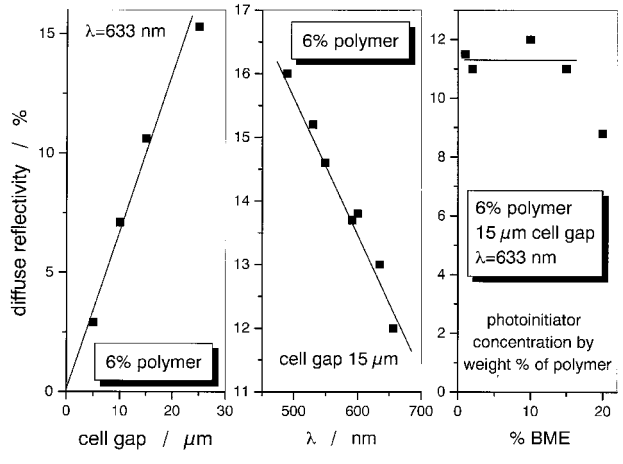

Fig. 8. Dependence of the diffuse reflectivity on cell gap, wavelength, and concentration of photoinitiator.

2.4.2. Polymerization Conditions and Network Morphology

The network morphology, usually imaged by SEM, does to some extent depend on the liquid-crystalline phase in which the polymerization is carried out.[35,46,47] Nevertheless, the following considerations are of a quite general nature and can be transferred to networks obtained not only in the cholesteric phase.

Monomer Concentration: Generally, two distinct polymer network morphologies are observed by photopolymerization in an LC medium:[34,48] rice grain–like structures and smooth polymer strands, as shown in Figure 9. Sometimes, especially when the polymerization is carried out in the isotropic phase of the LC, ball-like or plate-like structures are also observed.[49,50] It was often argued that the network morphology is due to the nature of the functional moiety and the flexibility of the chains attached to the mesogenic core. However, there is no evidence for this interpretation. We have modified the molecular structure of a monomer, which at a concentration of 6 wt.-% resulted in rice grain–like structures, in such a way that only the hydrogen atoms attached to the phenyl rings were replaced by fluorine, preserving the nature of the functional moiety as well as the chain flexibility. Polymerization of this new monomer at

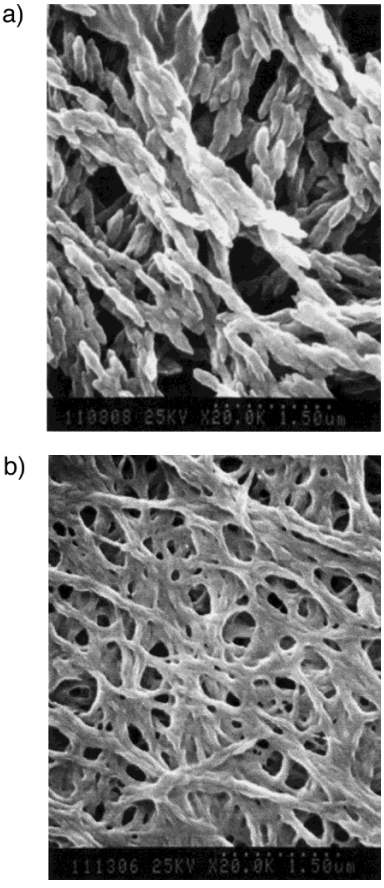

Fig. 9. General polymer network morphologies observed by SEM: a) rice grain–like structures for poor solubility and b) smooth network strands for good solubility of the monomer within the LC matrix.

  0935-9648/00/0302-0172 $ 17.50+.50/0

ADVANCED MATERIALS

the same concentration resulted in smooth network strands.[48] By changing the monomer content from a very low to a very high concentration (beyond usability in PSCT applications), it was shown for several different monomers that a crossover from a smooth to a grainy structure can be achieved (Fig. 10).[48] This behavior can be attributed to the solubility of the monomer within the LC. Poorly soluble monomers, close to the solubility limit, undergo a precipitation polymerization, whereas highly soluble monomers, well below the solubility limit, undergo a radical chain polymerization, leading to smooth networks. The behavior may be understood in the context of the Flory–Huggins model of polymer solubility, which is the primary factor determining the network morphology. Generally, increasing monomer concentration leads to denser polymer networks with smaller voids.[51,52]

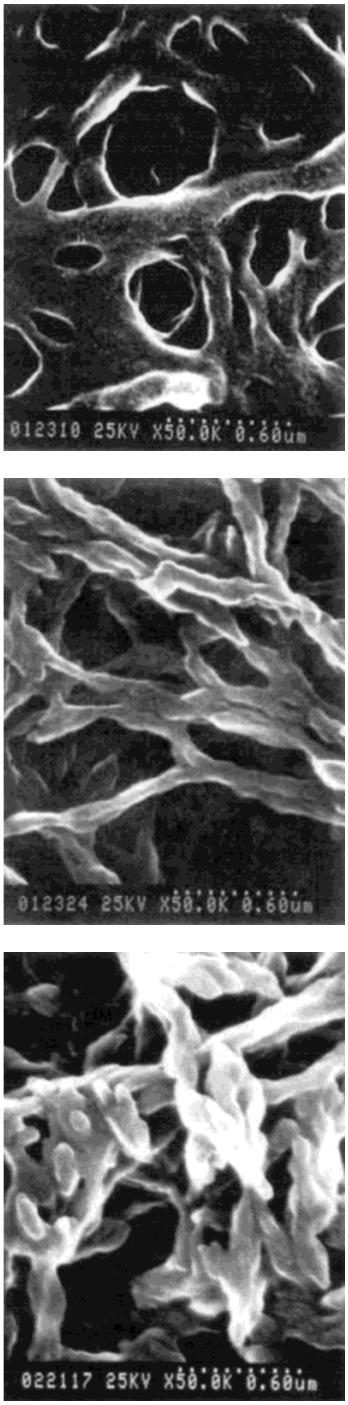

Fig. 10. Crossover from a smooth to rice grain–like morphology on increasing monomer concentration: a) 0.7 %, b) 1.5 %, c) 4 %, illustrating the effect of monomer solubility on the network morphology.

At this point it should be mentioned that rice grain–like structures generally lead to PSCTs with lower driving voltage, but also lower reflectivity as well as longer response times for the field-off texture reorientation. In contrast, smoothly structured networks lead to higher reflectivity and fast response times and also to considerably higher threshold fields. This behavior is demonstrated in Figure 11 for the electric field dependence of the reflectivity of two

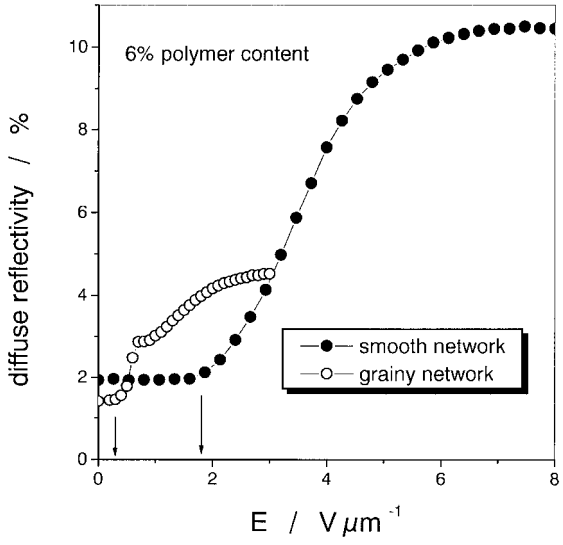

Fig. 11. Comparison of PSCTs with a smooth and a grainy network morphology (depending on the monomer used), prepared under identical conditions. Grainy networks exhibit small reflectivity at low driving voltages, while smooth networks lead to larger reflectivity with strongly increased threshold field (see arrows).

networks prepared under identical conditions from two different monomers. The residual back-scattering of both systems in the field-free state is approximately equal (~2 %). While for the grainy network (Fig. 9a) the texture transition already sets in at about E_{th} = 0.2 V μm^{-1}, the system with the smoothly stranded network (Fig. 9b) exhibits a threshold field that is an order of magnitude larger. The maximum achieved reflectivity of the smooth network is more than twice as large as that observed for the grainy network morphology.

For increasing monomer concentration an increase of reflectivity until saturation is observed, while the diffuse transmittance (off-specular forward scattering) decreases. The threshold field strongly increases with increasing network content and the response times for the reorientation back to the zero-field texture become faster. Exemplary data of the dependence of these principal electro-optical performance parameters on polymer concentration are de-

  0935-9648/00/0302-0173 $ 17.50+.50/0

picted in Figure 12. The behavior can be correlated with an increasing network density, as observed by SEM investiga-

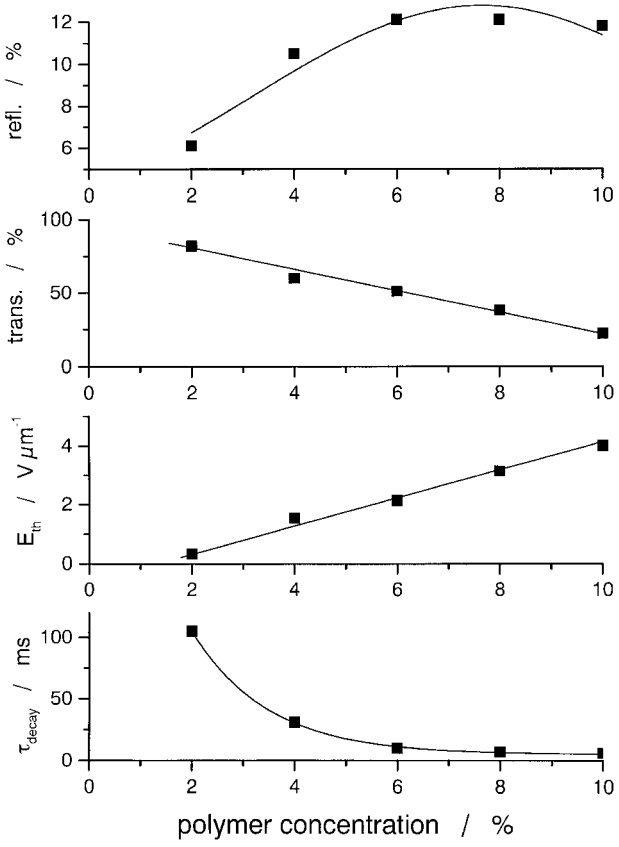

Fig. 12. Dependence of the reflectivity, transmittance, threshold field, and response time (scattering to transparent) on the concentration of polymer network. All cells were prepared under otherwise identical conditions (same cell gap $d = 15$ µm, curing temperature $T = 25$ °C, UV intensity 0.5 mW cm^{-2}, and time of UV exposure 5.5 h).

tions, and thus stronger elastic interactions between the network and the liquid-crystalline material.[51,53,54] In non-stabilized cholesterics the critical field for the texture transition (helix unwinding) is basically proportional to the square root of the ratio between the elastic constant K and the dielectric anisotropy $\Delta\varepsilon$: $E_C \sim (K/\Delta\varepsilon)^{1/2}$. In network-stabilized samples this quantity, and similarly the threshold voltage, should be modified by an additional term, which is proportional to an interaction constant between the network and LC and which in turn is a function of polymer concentration. Analogously, the reorientation time τ_{decay} (scattering to transparent) for non-stabilized cholesterics is proportional to the ratio of the viscosity γ to the elastic constant K: $\tau_{decay} \sim \gamma/K$, and is thus independent of the applied electric field. For stabilized samples, τ_{decay} should also be modified by a term inversely proportional to an interaction constant. The polymer network thus acts like an effective elastic field, having the same effect as an increase of the (twist) elastic constant.

Curing Temperature:[49,55] Also the temperature at which the polymerization is carried out has a profound influence on the network morphology and thus the electro-optical performance of the PSCT. The morphology of individual polymer strands, which varies significantly for different monomers used, remains largely unchanged. This means that the solubility of the monomer within the LC is not dramatically changed in the temperature range under investigation (–10 to 60 °C). We do not observe a crossover from smooth to grainy structures only by variation of curing temperature, but the average void size of the network increases as the temperature is raised; this has been imaged by SEM. The density of the network thus decreases for increasing polymerization temperature. Along with this change in morphology a decrease in reflectivity and threshold voltage is observed, while the diffuse transmittance increases. As expected, the response time for the field-on texture transition (transparent to scattering) remains constant, as this is a dielectrically driven process. The transition from the scattering to the transparent state after field removal, which is an elastically driven process, shows strongly increasing response times with increasing network mesh size obtained by increasing curing temperature. Exemplary data of the dependence of some important electro-optical parameters on curing temperature are summarized in Figure 13.

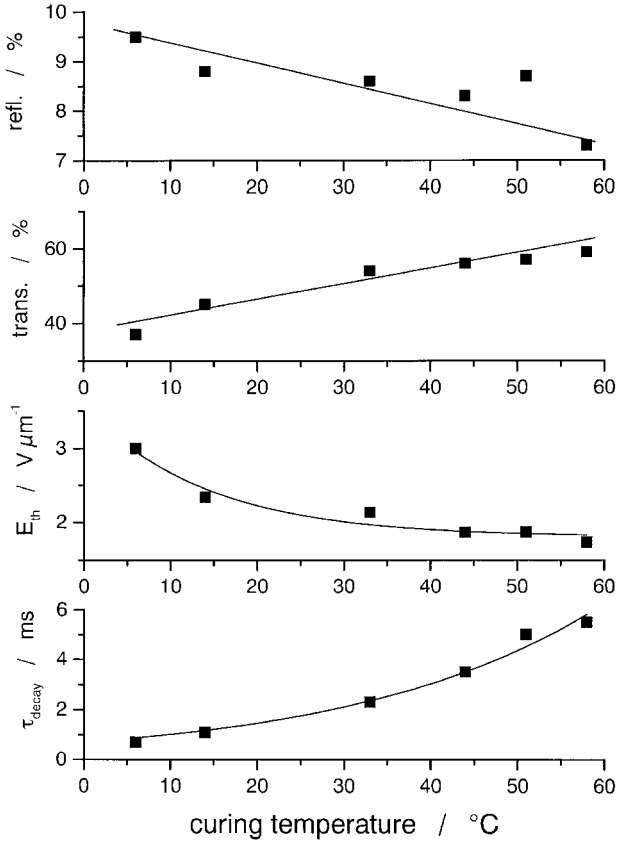

Fig. 13. Dependence of the reflectivity, transmittance, threshold field, and response time (scattering to transparent) on curing temperature during photopolymerization. All cells were prepared under otherwise identical conditions (same cell gap $d = 15$ µm, monomer concentration 6/wt.-%, UV intensity 0.5 mW cm^{-2}, and time of UV exposure 5.5 h).

UV Conditions:[34,56] The UV conditions of the photopolymerization process can be varied either by variation of

  0935-9648/00/0302-0174 $ 17.50+.50/0

ADVANCED MATERIALS

the UV intensity or the time of UV irradiation. Variation of the UV intensity in the range between 0.01 and 10 mW cm^{-2} does not have a pronounced effect on the network morphology, only slightly increasing the network void size for increasing intensity. Thus also the electro-optical performance remains largely unchanged, exhibiting a slightly decreasing reflectivity and threshold voltage for increasing UV intensity, while the transmittance and response times increase.

In contrast, the time of UV irradiation has a drastic effect on the network morphology, especially during the first hour of exposure.[56] From our electro-optical and SEM investigations we conclude that the polymerization process is completed after approximately 30–60 min. A strongly decreasing network void size is observed for increasing time of irradiation, indicating that the polymerization process is proceeding with time. Along with this solidification of the network a greatly increasing reflectivity, decreasing transmittance, increasing threshold voltage, and decreasing response time for the field-off texture transition are observed. Also here we depict some exemplary data of the electro-optical parameters (Fig. 14). In this special case the response time for the field-on texture transition is not constant, but increases for increasing time of UV irradiation

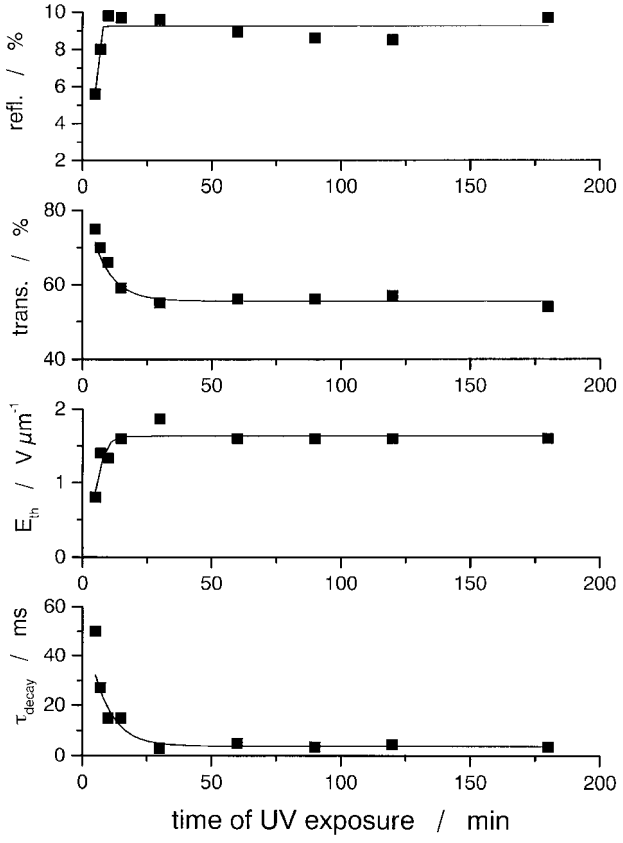

Fig. 14. Dependence of the reflectivity, transmittance, threshold field, and response time (scattering to transparent) on time of UV exposure. All cells were prepared under otherwise identical conditions (same cell gap d = 15 μm, curing temperature T = 25 °C, monomer concentration 6 wt.-%, UV intensity 0.5 mW cm^{-2}).

until saturation after approximately 1 h. This can be attributed to an increasing viscosity as oligomers and short-chain polymers are formed, while still being dissolved in the LC, before, at longer polymerization times, phase separation occurs.

2.4.3. Transfer of Helical Cholesteric Order onto the Network

SEM: As pointed out above, the general idea of polymer network–stabilized liquid crystals is to template the liquid-crystalline order by transferring the respective structure and orientation onto the network during polymerization. In order to investigate a transfer of the helical cholesteric order a novel preparation technique for SEM samples was developed,[57] allowing controlled resolution through the bulk of the cell, without deformation of the network during sample preparation. Conventional preparation techniques consist of breaking or cutting the sample and removal of the LC by a solvent to expose the polymer network. This may distort the fragile network structure and usually does not allow a controlled depth profile. For our novel technique, the LC is also removed by immersing the cell in a suitable organic solvent (generally ether) for several days. The cells are then placed in a pressure chamber and the ether replaced by liquid CO_2, which is subsequently brought through its critical point into the gaseous state, resulting in dry, solvent-free cells. This procedure avoids any distortion of the polymer structure due to surface tension effects as the solvent dries.[58] In a next preparation step the network is encapsulated using a reworkable epoxy. The cell with the polymer network is refilled by a liquid epoxy polymer precursor and thermally cured. It can then be ground at a small angle and polished to a mirror smooth finish to expose the epoxy-encapsulated polymer network. At this wedge the epoxy is subsequently removed by an acid, which leaves a layer of the unperturbed polymer network to be coated by a thin film of AuPd for SEM imaging. These samples allow a controlled depth profile through the bulk of the cell.

Using samples prepared in such a way, the helical superstructure of the polymer network formed in the cholesteric phase can clearly be imaged, as shown in Figure 15.[51] Samples of cell gap 15 μm prepared with a chiral nematic of pitch 10 μm, clearly exhibited three π-twists between the top and the bottom substrate.[51] Below, we will discuss the importance of the helical transfer in more detail.

Confocal Microscopy: The use of confocal microscopy allows in-situ confirmation of the transfer of the cholesteric helix onto the polymer network[59] by moving the focal plane through the bulk of the sample at a resolution of approximately 0.2 μm. For these investigations the polymer network within the LC is tagged with a fluorophore and the fluorescent image recorded, with bright regions of the image corresponding to the polymer network. An illustrative example is given in Figure 16, with images taken at

  0935-9648/00/0302-0175 $ 17.50+.50/0

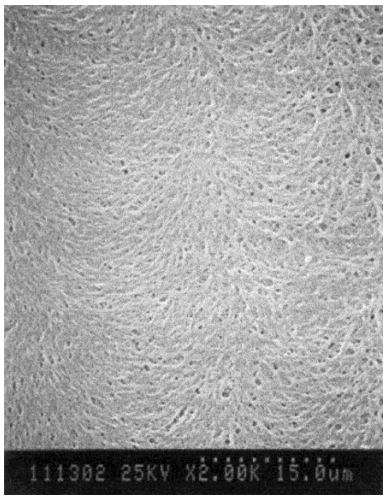

Fig. 15. SEM image of a polymer network formed in the chiral nematic phase. A transfer of the helical superstructure of the LC onto the polymer network can clearly be seen.

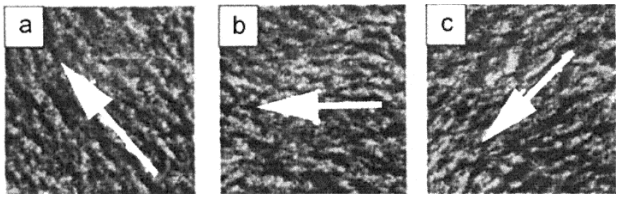

Fig. 16. Confocal microscopy images of a fluorescently tagged polymer network formed in the chiral nematic phase. The average preferred direction of the network changes as the focal plane is lowered through the bulk of the sample (a–c), indicating a helical structure of the polymer network with helical axis perpendicular to the substrates. (Image size: 25 μm × 25 μm, bright regions correspond to polymer network).

planes separated by 1 μm through the volume of the cell. For each image one can clearly detect a preferred direction of the polymer network, corresponding to local nematic order. As the focal plane is moved through the sample this direction changes, indicating a helical superstructure. In fact, an angular difference of approximately 35° is observed over a depth change of 1 μm, exactly corresponding to the adjusted pitch of 10 μm.[59]

2.4.4. Two-Step Texture Reorientation

Electro-optical Behavior and Network Morphology: For some PSCTs the texture reorientation between the planar, transparent, and focal-conic scattering state is accomplished via a two-step process, as can be seen in the diffuse reflectivity (Fig. 17a) as well as in the dynamic response after field removal (Fig. 17b). This behavior is closely linked to the network morphology and especially the polymer network void size. A two-step texture reorientation is generally observed for large mesh sizes and rice grain–like morphologies, and thus for poor solubility of the monomer within the LC, decreasing monomer concentration, increasing curing temperature, large UV curing intensities, and short UV exposure times. For these fabrication parameters

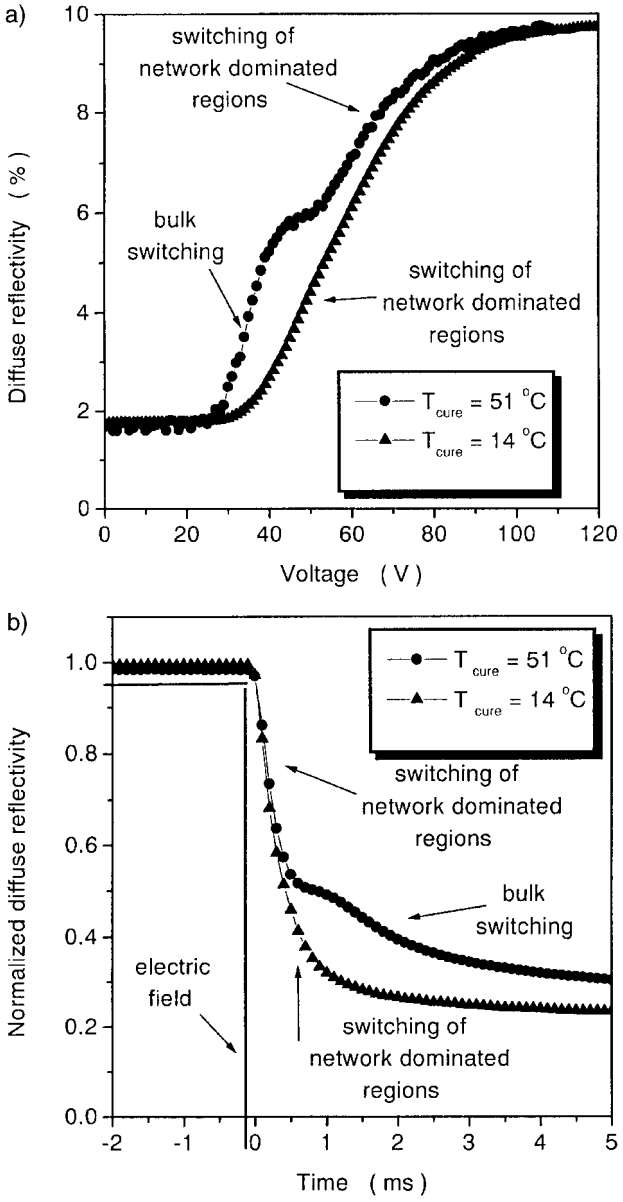

Fig. 17. Two-step texture transition (●) for networks with large voids (formed at elevated polymerization temperatures) and single-step transition (▲) for networks with small voids (formed at low polymerization temperatures) as observed in a) the static as well as b) the dynamic response of the diffuse reflectivity.

an increasing void size is observed and passing a critical (average) network mesh dimension on the order of 0.5 μm, two-step switching appears. This value has been estimated from SEM studies for all of the investigation series mentioned above (for the given LC and monomer material). The behavior is attributed to the cholesteric LC being divided into two distinct environments: bulk-like material and strongly network-dominated regions.[51] For large voids the enclosed LC behaves bulk-like, leading to a reorientation process at low threshold voltage with long decay time in the dynamic response. Small voids enclose LC material that is strongly dominated by elastic interaction with the polymer network. This leads to high threshold switching

  0935-9648/00/0302-0176 $ 17.50+.50/0

ADVANCED MATERIALS

and a fast reorientation back to the planar state when the electric field is removed. As, due to preparation conditions, the void size is reduced (high monomer content, low curing temperature, moderate UV intensities, and long irradiation time), two-step switching vanishes and only a one-stage switching transition is observed at large threshold with fast response time for the field-off texture transition. In this case all LC material is dominated by the influence of the polymer network. It is interesting to note that, for all systems with a smooth network morphology, i.e., highly soluble monomers, the appearance of the single-step texture transition is accompanied by a transfer of the helical cholesteric order onto the polymer network, while for two-step switching a transfer of the helical order cannot be observed.

In-situ Confocal Microscopy: The phenomenological explanation for the two-step reorientation was evidenced by confocal microscopy studies on samples of a fluorescently tagged polymer network.[59] It could clearly be shown that regions with little polymer content (large voids) exhibit switching at much lower voltages than regions with a large polymer concentration (small voids), as demonstrated in Figure 18. The behavior was directly correlated to the electro-optical performance of the cell. A random-field model accounts for a qualitative theoretical description of the two-step texture reorientation.[59]

2.4.5. Applications

Scattering Devices with Long-Pitch Cholesterics: The general mode of operation of scattering devices based on long-pitch cholesterics has been outlined above. For reverse-mode as well as normal-mode PSCTs the switching is based on a texture transition between a transparent and a scattering state.[45] The stabilization of the initial field-free texture by the polymer network is needed to cause a rapid reorientation back to this state after removal of the electric field. The currently achieved values for the reflectivity of ap-

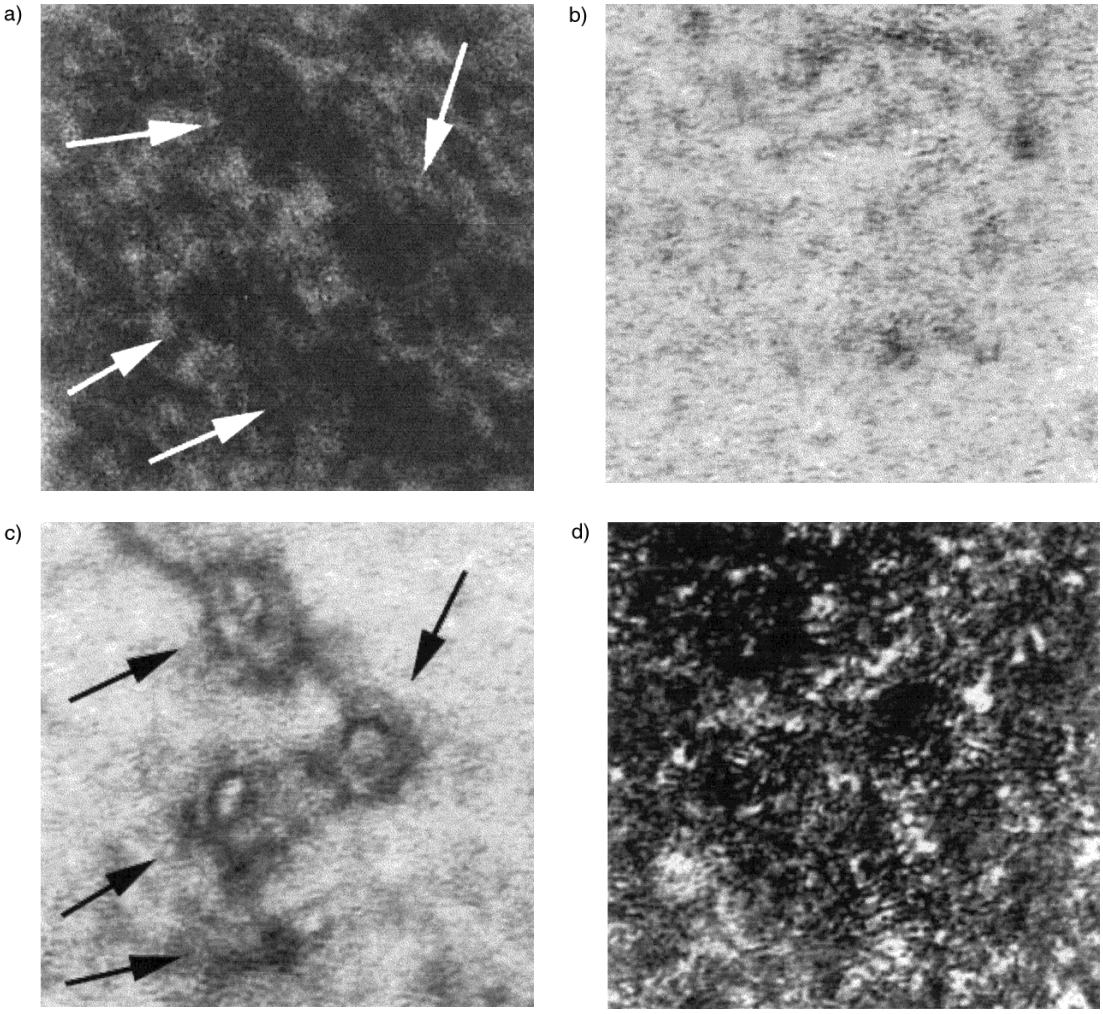

Fig. 18. a) Confocal microscopy image of the PSCT in the fluorescent mode (bright regions are polymer rich). Large voids can be observed, indicated by arrows in the image. b) Corresponding image in the scattering mode with no electric field applied. c) Scattering mode image at moderate voltages shows the texture transition starting in regions of large voids (bulk switching). d) At larger voltages the second reorientation step is observed (switching of polymer-dominated regions). (Image size: 25 μm × 25 μm.)

  0935-9648/00/0302-0177 $ 17.50+.50/0

proximately 25 % are still too low for a sufficient contrast ratio and, moreover, the driving voltages to achieve these values are presently still too high to allow for a portable, low-power display.

Reflective Devices with Short-Pitch Cholesterics: Another possibility for achieving high reflectivity (50 % in theory) is the use of devices based on the selective reflection of a short-pitch cholesteric, stabilized by a polymer network.[60] If the pitch P of the cholesteric is on the order of several hundred nanometers, thus in the range of the visible spectrum, and oriented with the helical axis in the direction of light propagation, a reflection of circularly polarized light at a wavelength of $\lambda_0 = \bar{n}P$ is observed, where $\bar{n}$ is an average index of refraction. Here, the reflectivity due to scattering in the field-on state should be small, which can be achieved by scattering from large focal-conic domains. With a black background, the device switches from brightly colored (λ_0) at zero field to black at applied electric fields. First bi-stable prototypes with good contrast and viewing angle have been demonstrated by Kent Display Systems.[61–63] Scattering and the effect on the pitch of short-pitch polymer-stabilized cholesterics have been studied[64,65] and photometric and colorimetric properties have been reported.[66]

Another interesting, though very different approach, lies in the flexoelectro-optical effect,[67] where a short-pitch cholesteric is oriented uniformly and unidirectionally with its helical axis (which is at the same time the optical axis) in the plane of the substrate. Such an arrangement behaves like a birefringent plate as the helical structure cannot be resolved optically. Application of an electric field perpendicular to the helical axis results in a linear deflection of the optical axis in the plane of the substrate, thus achieving gray-scale displays when placed between crossed polarizers. One problem faced in the fabrication of those devices is the degradation of the liquid-crystalline orientation with time. Recently, it was shown[68] that this orientation can be greatly enhanced and stabilized by the incorporation of a polymer network without profound changes of the electro-optical performance as compared to the unstabilized system.

2.5. Polymer Network–Stabilized Ferroelectric Liquid Crystals

From symmetry considerations[1] it follows that tilted smectic phases, composed of chiral molecules, exhibit a spontaneous polarization. If the direction of this polarization can be reversed by an electric field, as is the case for SmC* materials, we speak of (improper) FLCs. Bi-stable switching is achieved when the helical superstructure of the SmC* phase is unwound by surface interactions between the LC and the substrate,[69] usually when the cell gap becomes smaller than the SmC* pitch. The most desirable orientation from the applicational point of view, i.e., which allows the greatest contrast, is the so-called bookshelf geometry with the smectic layers oriented perpendicular to the substrate. On application of an electric field the optical axis reorients on the tilt cone between two stable states. Switching is intrinsically bi-stable and response times are quite fast, on the order of several microseconds, so that video-rate displays can be achieved, in contrast to conventional nematics. Nevertheless, application of FLCs poses some considerable technical problems as they have to be used in very thin cells (on the order of 2 μm) and the needed uniform molecular orientation is not as readily achieved as for nematics. Furthermore, the smectic layer structure possesses only low resistivity to mechanical shock, without the self-healing effect of a nematic display. In the light of these problems it was proposed that the smectic layer orientation could be stabilized by polymer networks.[70] Samples were prepared as outlined above, except that the polymerization was carried out in the SmC* phase. Again, the polymer network follows the liquid-crystalline orientation and thus stabilizes the polar order of SmC* as evidenced by piezoelectric measurements.[71]

2.5.1. Effect on Physical Parameters

In general, the introduction of a polymer network has a considerable influence on the physical parameters and the electro-optical behavior of the SmC* phase as compared to the pure LC material.[72] When using a polymer with a smaller birefringence than that of the LC, the effective birefringence usually decreases with increasing network concentration.[73] This is in fact an effect that is desirable for display production, as it allows one to work with larger cell gaps. The tilt angle, which is half of the switching angle of the FLC device, is an important parameter because the electro-optical response (intensity modulation, contrast ratio) is closely related to the value of the tilt. The effective tilt angle of the stabilized FLC was reported to decrease with increasing network density and to be smaller than for the pure FLC.[73,74] This is attributed to different microscopic regions within the sample: those that switch with the same tilt as the pure FLC (bulk switching, compare to PSCTs) and regions in the vicinity of the network strands that do not switch at all or only with a smaller tilt angle. The measured effective tilt is an average of the two regions. In contrast to non-stabilized samples, the effective tilt is strongly dependent on applied voltage, having a profound impact on the transmission–voltage characteristic of the cell[73,75] and allowing gray-scale generation with a device that is otherwise (in the non-stabilized state) bi-stable, thus allowing only monochrome information display.

A similar behavior was reported for the spontaneous polarization, which is found to be smaller than for the pure FLC and decreases with increasing polymer concentration,[73,74] as exemplarily depicted in Figure 19. From this data, it is clear that the reduction of the spontaneous polarization is not solely due to dilution, which is a minor effect

  0935-9648/00/0302-0178 $ 17.50+.50/0

ADVANCED MATERIALS

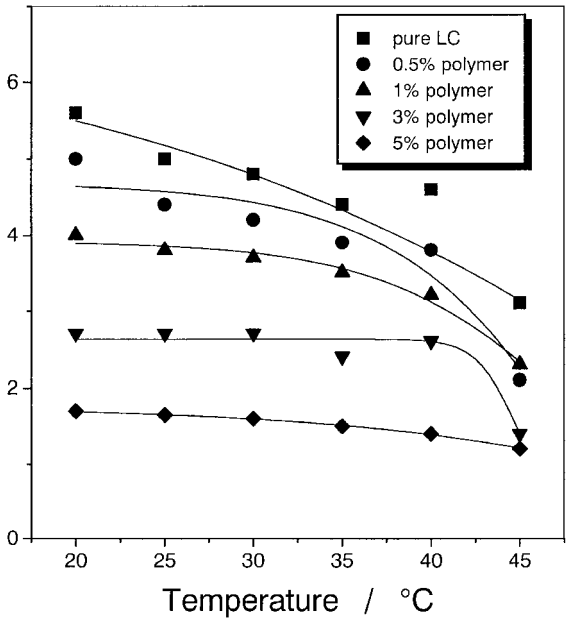

Fig. 19. Temperature dependence of the spontaneous polarization, P_S, as a function of polymer network concentration (data after [74]).

at these low network concentrations. Effects of UV curing conditions on the polarization behavior have been pointed out.[76] The current reversal peak is smeared out and reduced for increasing network content.[73] Electro-optical response times are increasing for increasing polymer concentration, but drastic effects are not observed.[74] As the response time, τ, and spontaneous polarization, P_S, are closely linked to the rotational viscosity, γ, by the relation $\tau \approx \gamma/P_S E$, this might explain the observed decrease of the rotational viscosity reported for increasing network concentration.[74]

It should also be pointed out that the introduction of a polymer network has an influence on the local phase symmetry of the liquid-crystalline material in the vicinity of the transition from the ferroelectric SmC* to the paraelectric SmA* phase, depending on the phase in which the polymerization was carried out.[77] Polymerization at large tilt angles in the SmC* phase tends to preserve the tilted order close to the network strands, which causes a contribution to the spontaneous polarization even when the bulk transition to the SmA* phase has occurred. In analogy, polymerization at zero tilt in the SmA* phase tends to preserve orthogonal order, resulting in a reduction of the spontaneous polarization as the bulk transition to SmC* is crossed. This behavior can theoretically be explained by an effective field due to the polymer network, where the interaction parameter between the network and the LC was found to be linearly dependent on polymer concentration.[77]

2.5.2. Electro-optical Performance

The electro-optical performance of network-stabilized FLCs is generally found to be decreased to some extend with respect to effective switching angle, spontaneous polarization, and response time. Nevertheless, this should not obscure the applicational advantages as, compared to nematic devices, the switching speed is still fast, good contrast ratios may be obtained, and mechanical stabilization may be achieved. This becomes increasingly evident when effects such as smectic layer directional instability[78–80] under application of asymmetric electric fields (as they are usually applied in display driving schemes) are discussed. It has been shown that the applicationally undesirable reorientation of the smectic layer normal under asymmetric electric fields can be suppressed by the introduction of a polymer network,[81,82] stabilizing a uniform smectic layer and director configuration.

When the polymerization is carried out under direct current (DC) field conditions, thus selecting one of the stable ferroelectric states, again the network follows the molecular orientation and stabilizes the selected state. This leads to an asymmetric electro-optical response and different response times for switching with opposite field polarity,[83] similar to the behavior described for weakly crosslinked ferroelectric elastomers.[84]

2.6. Polymer Network–Stabilized Antiferroelectric Liquid Crystals

Antiferroelectric order in chiral LCs[85] was demonstrated some years ago and their interesting applicational aspects are currently being explored worldwide. At zero field an anticlinical orientation of the molecules in adjacent layers is observed. Under application of electric fields of sufficient amplitude, switching into one of the two ferroelectric states is achieved, depending on the polarity of the field. Antiferroelectric liquid crystals (AFLCs) thus exhibit monostable, tri-state switching. An account of investigations on polymer-stabilized AFLCs has been given in the literature.[86] Introduction of a polymer network of low concentration, formed at zero voltage in the antiferroelectric state, does maintain the optical and electrical double-hysteresis characteristic of AFLCs, while at the same time the threshold for the field-induced antiferroelectric to ferroelectric transition is smeared out with increasing polymer concentration. It has been pointed out that this non-uniformity of the threshold field can effectively be used to generate gray levels under realistic driving sequences used in the addressing of AFLC displays.[87] As expected from the behavior of network-stabilized FLCs, also for AFLCs the introduction of a polymer network decreases the effective tilt angle, θ, as well as the spontaneous polarization, P_S, with increasing polymer concentration, while the dynamic behavior (response times) remains basically unchanged.[86]

3. Summary

The fabrication, structure, and electro-optical performance of PSLCs have been reviewed. Fundamental aspects

  0935-9648/00/0302-0179 $ 17.50+.50/0

of the polymer network formation in an anisotropic medium were pointed out and the application potential was discussed for nematic, cholesteric, ferroelectric, and antiferroelectric SmC* LCs. Putting an emphasis on PSCTs, it was shown that the electro-optical performance strongly depends on the network morphology, which in turn is greatly influenced by processing conditions, such as polymer concentration, curing temperature, UV curing intensity, and time of UV exposure.

Received: August 24, 1999
Final version: November 3, 1999

[1] R. B. Meyer, L. Liebert, L. Strzelecki, P. Keller, *J. Phys. Lett.* **1975**, *36*, L69.
[2] *Physical Properties of Liquid Crystals* (Eds: D. Demus, J. Goodby, G. W. Gray, H.-W. Spiess, V. Vill), Wiley-VCH, Weinheim **1999**. *Handbook of Liquid Crystals* (Eds: D. Demus, J. Goodby, G. W. Gray, H.-W. Spiess, V. Vill), Wiley-VCH, Weinheim **1998**.
[3] P. Collings, M. Hird, *Introduction to Liquid Crystal Chemistry and Physics*, Taylor and Francis, London **1997**.
[4] *Liquid Crystals* (Ed: H. Stegemeyer), Steinkopf, Darmstadt **1994**.
[5] P. G. deGennes, J. Prost, *The Physics of Liquid Crystals*, 2nd ed., Clarendon, Oxford **1993**.
[6] S. Chandrasekhar, *Liquid Crystals*, 2nd ed., Cambridge University Press, Cambridge **1992**.
[7] P. S. Drzaic, *Liquid Crystal Dispersions*, World Scientific, Singapore **1995**.
[8] G. P. Crawford, S. Zumer, *Liquid Crystals in Complex Geometries*, Taylor and Francis, London **1996**.
[9] J. L. Fergason, *US Patent 4 435 047*, **1984**. J. L. Fergason, *SID Int. Symp. Dig. Tech. Pap.* **1985**, *16*, 68.
[10] P. S. Drzaic, *J. Appl. Phys.* **1986**, *60*, 2142.
[11] J. W. Doane, N. A. Vaz, B. G. Wu, S. Zumer, *Appl. Phys. Lett.* **1986**, *48*, 269.
[12] J. L. West, *Mol. Cryst. Liq. Cryst.* **1988**, *157*, 427.
[13] B.-G. Wu, J. L. West, J. W. Doane, *J. Appl. Phys.* **1987**, *62*, 3925.
[14] N. A. Vaz, G. W. Smith, G. P. Montgomery, *Mol. Cryst. Liq. Cryst.* **1987**, *146*, 1.
[15] J. Y. Kim, P. Palffy-Muhoray, *Mol. Cryst. Liq. Cryst.* **1991**, *203*, 93.
[16] G. W. Smith, *Mol. Cryst. Liq. Cryst.* **1994**, *239*, 63.
[17] A. Golemme, G. Arabia, G. Chidichimo, *Mol. Cryst. Liq. Cryst.* **1994**, *243*, 185.
[18] A. Golemme, S. Zumer, D. W. Allender, J. W. Doane, *Phys. Rev. Lett.* **1988**, *61*, 2937.
[19] J. W. Doane, G. Chidishimo, N. A. Vaz, *US Patent 4 688 900*, **1987**. J. W. Doane, A. Golemme, J. L. West, J. B. Whitehead, B.-G. Wu, *Mol. Cryst. Liq. Cryst.* **1988**, *165*, 511.
[20] P. P. Crooker, D.-K. Yang, *Appl. Phys. Lett.* **1990**, *57*, 2529.
[21] H.-S. Kitzerow, H. Molsen, G. Heppke, *Appl. Phys. Lett.* **1992**, *60*, 3093.
[22] H.-S. Kitzerow, *Liq. Cryst.* **1994**, *16*, 1.
[23] L. Bouteiller, P. Le Barny, *Liq. Cryst.* **1996**, *21*, 157.
[24] D. J. Broer, H. Finkelmann, K. Kondo, *Makromol. Chem.* **1988**, *189*, 185.
[25] D. J. Broer, G. N. Mol, G. Challa, *Makromol. Chem.* **1989**, *190*, 19.
[26] D. J. Broer, J. Boven, G. N. Mol, G. Challa, *Makromol. Chem.* **1989**, *190*, 2255.
[27] D. J. Broer, R. A. M. Hikmet, G. Challa, *Makromol. Chem.* **1989**, *190*, 3201.
[28] D. J. Broer, G. N. Mol, G. Challa, *Makromol. Chem.* **1991**, *192*, 59.
[29] A. Jakli, L. Bata, K. Fodor-Csorba, L. Rostas, L. Noirez, *Liq. Cryst.* **1994**, *17*, 227.
[30] R. A. M. Hikmet, *J. Appl. Phys.* **1990**, *68*, 4406.
[31] R. A. M. Hikmet, *Liq. Cryst.* **1991**, *9*, 405.
[32] R. A. M. Hikmet, *Mol. Cryst. Liq. Cryst.* **1992**, *213*, 117.
[33] R. A. M. Hikmet, *Adv. Mater.* **1992**, *4*, 679.
[34] Y. K. Fung, D.-K. Yang, S. Ying, L.-C. Chien, S. Zumer, J. W. Doane, *Liq. Cryst.* **1995**, *19*, 797.
[35] A. Y.-G. Fuh, M.-S. Tsai, C.-Y. Huang, *Jpn. J. Appl. Phys.* **1996**, *35*, 3960.
[36] Y. K. Fung, A. Borstnik, S. Zumer, D.-K. Yang, J. W. Doane, *Phys. Rev. E* **1997**, *55*, 1637.
[37] R. E. Kraig, P. L. Taylor, R. Ma, D.-K. Yang, *Phys. Rev. E* **1998**, *58*, 4594.
[38] R. Stannarius, G. P. Crawford, L.-C. Chien, J. W. Doane, *J. Appl. Phys.* **1991**, *70*, 135.
[39] A. Riede, S. Grande, A. Hohmuth, W. Weissflog, *Liq. Cryst.* **1997**, *22*, 157.
[40] A. Jakli, D. R. Kim, L.-C. Chien, A. Saupe, *J. Appl. Phys.* **1992**, *72*, 3161.
[41] R. A. M. Hikmet, B. H. Zwerver, *Liq. Cryst.* **1991**, *10*, 835.
[42] R. A. M. Hikmet, R. Howard, *Phys. Rev. E* **1993**, *48*, 2752.
[43] P. Bos, J. Rahman, J. W. Doane, *SID Dig. Tech. Pap. XXIV* **1993**, 887.
[44] D. S. Fredley, B. M. Quinn, P. J. Bos, *Conf. Rec. IDRC* **1994**, 480.
[45] D.-K. Yang, L.-C. Chien, J. W. Doane, *Appl. Phys. Lett.* **1992**, *60*, 3102.
[46] C. V. Rajaram, S. D. Hudson, L.-C. Chien, *Chem. Mater.* **1995**, *7*, 2300.
[47] D. S. Muzic, C. V. Rajaram, L.-C. Chien, S. D. Hudson, *Polym. Adv. Technol.* **1996**, *7*, 737.
[48] I. Dierking, L. L. Kosbar, A. Afzali-Ardakani, A. C. Lowe, G. A. Held, *Appl. Phys. Lett.* **1997**, *71*, 2454.
[49] C. V. Rajaram, S. D. Hudson, L.-C. Chien, *Chem. Mater.* **1996**, *8*, 2451.
[50] C. V. Rajaram, S. D. Hudson, L.-C. Chien, *Polymer* **1998**, *39*, 5315.
[51] I. Dierking, L. L. Kosbar, A. Afzali-Ardakani, A. C. Lowe, G. A. Held, *J. Appl. Phys.* **1997**, *81*, 3007.
[52] M. Mitov, A. Boudet, P. Sopena, P. Sixou, *Liq. Cryst.* **1997**, *23*, 903.
[53] D.-K. Yang, L.-C. Chien, Y. K. Fung, in *Liquid Crystals in Complex Geometries* (Eds: G. P. Crawford, S. Zumer), Taylor and Francis, London **1996**, Ch. 5.
[54] T. Nakata, T. Gotoh, M. Satoh, E. Hasegawa, *Mol. Cryst. Liq. Cryst.* **1997**, *299*, 389.
[55] I. Dierking, L. L. Kosbar, A. C. Lowe, G. A. Held, *Liq. Cryst.* **1998**, *24*, 387.
[56] I. Dierking, L. L. Kosbar, A. C. Lowe, G. A. Held, *Liq. Cryst.* **1998**, *24*, 397.
[57] I. Dierking, L. L. Kosbar, S. L. Buchwalter, unpublished.
[58] L. Bouteiller, P. LeBarny, P. Robin, J. C. Dubois, *Proc. 14th Int. Display Research Conf.*, Monterey, CA **1994**, p. 195.
[59] G. A. Held, L. L. Kosbar, I. Dierking, A. C. Lowe, G. Grinstein, V. Lee, R. D. Miller, *Phys. Rev. Lett.* **1997**, *79*, 3443.
[60] D.-K. Yang, J. L. West, L.-C. Chien, J. W. Doane, *J. Appl. Phys.* **1994**, *76*, 1331.
[61] J. L. West, G. R. Magyar, J. J. Francl, *Proc. SID* **1994**, 608.
[62] D.-K. Yang, J. W. Doane, Z. Yaniv, J. Glasser, *Appl. Phys. Lett.* **1994**, *64*, 1905.
[63] M. Pfeiffer, D.-K. Yang, J. W. Doane, R. Bunz, E. Lüder, M.-H. Lu, H. Yuan, C. Catchpole, Z. Yaniv, *SID 95 Dig.* **1995**, 706.
[64] R. A. M. Hikmet, B. H. Zwerver, *Liq. Cryst.* **1992**, *12*, 319.
[65] R. A. M. Hikmet, B. H. Zwerver, *Liq. Cryst.* **1993**, *13*, 561.
[66] W. D. St. John, Z.-J. Lu, J. W. Doane, B. Taheri, *J. Appl. Phys.* **1996**, *80*, 115.
[67] J. S. Patel, R. B. Meyer, *Phys. Rev. Lett.* **1987**, *58*, 1538.
[68] P. Rudquist, L. Komitov, S. T. Lagerwall, *Liq. Cryst.* **1998**, *24*, 329.
[69] N. A. Clark, S. T. Lagerwall, *Appl. Phys. Lett.* **1980**, *36*, 899.
[70] J. Pirs, R. Blinc, B. Marin, I. Musevic, S. Pirs, S. Zumer, J. W. Doane, poster C-P89, presented at *14th Int. Liquid Crystal Conf.*, Pisa, Italy, June 21–26, **1992**. J. Pirs, R. Blinc, B. Marin, S. Pirs, J. W. Doane, *Mol. Cryst. Liq. Cryst.* **1995**, *264*, 155.
[71] R. A. M. Hikmet, J. Lub, *J. Appl. Phys.* **1995**, *77*, 6234.
[72] R. A. M. Hikmet, M. Michielsen, *Adv. Mater.* **1995**, *7*, 300.
[73] R. A. M. Hikmet, H. M. J. Boots, M. Michielsen, *Liq. Cryst.* **1995**, *19*, 65.
[74] C. A. Guymon, E. N. Hoggan, D. M. Walba, N. A. Clark, C. N. Bowman, *Liq. Cryst.* **1995**, *19*, 719.
[75] J. Li, Z. Wang, Y. Cai, X. Huang, *Ferroelectrics* **1998**, *213*, 91.
[76] J. Nourry, A. Vigouroux, A. Magnaldo, P. Sixou, M. Mitov, A. Boudet, M. Glogarova, A. M. Bubnov, *Ferroelectrics* **1998**, *212*, 203.
[77] I. Dierking, M. A. Osipov, S. T. Lagerwall, unpublished.
[78] G. Andersson, T. Carlsson, S. T. Lagerwall, M. Matuszczyk, T. Matuszczyk, presented at *4th Int. Conf. on Ferroelectric Liquid Crystals*, Tokyo, Japan, Sept. 28–Oct. 1, **1993**.
[79] K. Nakayama, H. Moritake, M. Ozaki, K. Yoshino, *Jpn. J. Appl. Phys. Lett.* **1995**, *34*, L1599.
[80] I. Dierking, L. Komitov, S. T. Lagerwall, *Liq. Cryst.* **1998**, *24*, 775.
[81] H. Ishii-Erikson, *M.Sc. Thesis*, Chalmers University of Technology, Gothenburg, Sweden **1995**.
[82] I. Dierking, L. Komitov, S. T. Lagerwall, T. Wittig, R. Zentel, *Liq. Cryst.* **1999**, *26*, 1511.
[83] H.-S. Kitzerow, T. Röder, J. Strauss, poster PA11 presented at *7th Int. Conf. on Ferroelectric Liquid Crystals*, Darmstadt, Germany, Aug. 29–Sept. 3, **1999**.

  0935-9648/00/0302-0180 $ 17.50+.50/0

[84] M. Brehmer, R. Zentel, F. Gießelmann, R. Germer, P. Zugenmaier, *Liq. Cryst.* **1996**, *21*, 589.
[85] A. D. L. Chandani, T. Hagiwara, Y. Suzuki, Y. Ouchi, H. Takezoe, A. Fukuda, *Jpn. J. Appl. Phys. Lett.* **1988**, *27*, L729.
[86] J. Strauss, H.-S. Kitzerow, *Ber. Bunsenges. Phys. Chem.* **1998**, *102*, 1609.
[87] J. Strauss, H.-S. Kitzerow, *Appl. Phys. Lett.* **1996**, *69*, 725.

  0935-9648/00/0302-0181 $ 17.50+.50/0